Rainfall erosivity and sediment yield in Northeast Algeria: K'sob watershed case study

Mourad Guesri, Abdesselam Megnounif & Abderrahmane Nekkache Ghenim

Arabian Journal of Geosciences

ISSN 1866-7511
Volume 13
Number 7

Arab J Geosci (2020) 13:1-11
DOI 10.1007/s12517-020-5276-1

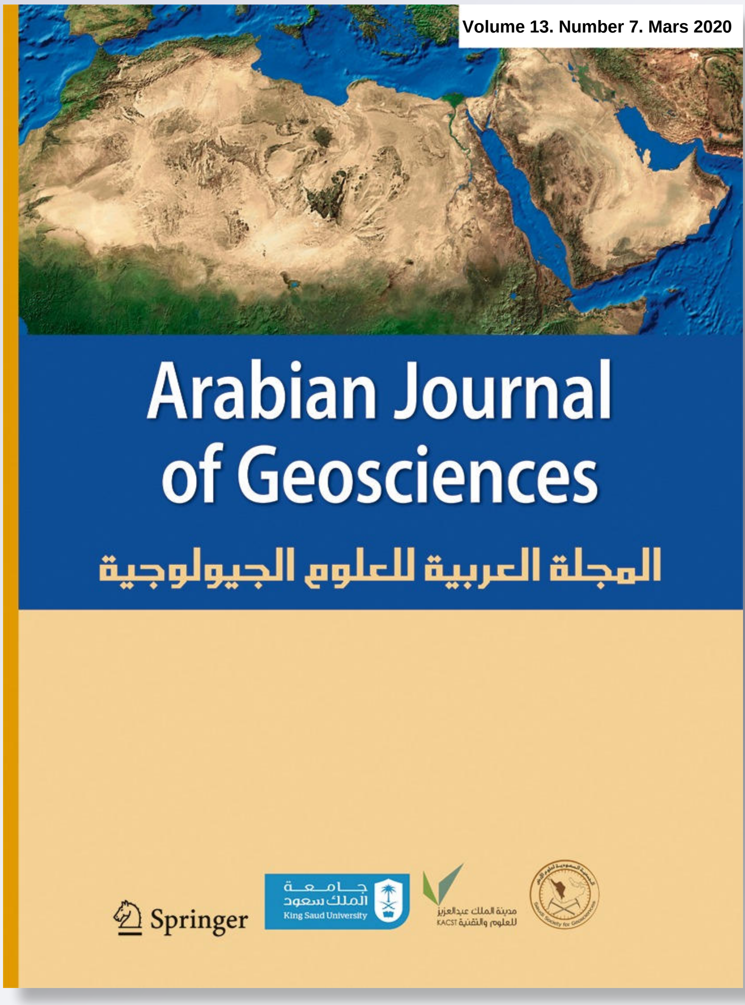

Springer

Arabian Journal of Geosciences (2020) 13:299
https://doi.org/10.1007/s12517-020-5276-1

ORIGINAL PAPER

Rainfall erosivity and sediment yield in Northeast Algeria: K'sob watershed case study

Mourad Guesri[1] · Abdesselam Megnounif[2] · Abderrahmane Nekkache Ghenim[2]

Received: 11 March 2019 / Accepted: 3 March 2020

Abstract

In semiarid areas, rainfall is often intense on dry soils with poor vegetation which might lead to high soil erosion susceptibility. Therefore, an appropriate assessment of the rainfall erosivity is of particular importance due to negative effects caused by top soil depletion and excessive sediment loading to receiving waters of reservoirs. The present study was conducted on the Wadi K'sob watershed (1480 km^2) in northeast Algeria with an aim to examine the rainfall erosivity. The calculation of such an index is based on rains exceeding a specific threshold and requires rainfall data with a fine temporal resolution, which, often, are rare or difficult to acquire. The examination of daily rains occurring before a flood event carrying sediment load showed a spatial variability of the thresholds of rainfall erosivity. The seasonal values of the thresholds are low and lying between 2 mm in summer and 6 mm in winter, highlighting an erosivity process characteristically high in semi-arid regions. Empirical relationships, established at seasonal scale, were proposed as an alternative solution to the R-index calculation derived from the Revised Soil Loss Equation. The determined models allowed us to simulate the erosivity of rainfall events as a function of daily rain. Between 68 and 78% of the variance of rainfall erosivity is explained by the daily rainfall giving rise to an erosive rainfall event. Then, the spatial mean of the annual erosivity index fluctuated between 228 and 386 MJ mm ha^{-1} h^{-1} year^{-1} with an interannual average of 302 MJ mm ha^{-1} h^{-1} year^{-1}, which if underestimated by 6%, the erosivity index quantified according to the Revised Universal Soil Loss Equation. Rainfall erosivity is the determining factor in sediment yield with a different degree of binding during the year. In autumn, 68% of the variance in sediment production is explained by rainfall erosivity, compared with only 42% in spring due to changes in soil conditions, including the presence of a vegetation cover that protects the soil against rainfall erosivity.

Keywords Rainfall · Erosivity index · Sediment transport · Semiarid · Wadi K'sob watershed · Northeast Algeria

Introduction

Rainfall erosivity has been studied extensively to understand soil erosion. In semiarid areas, generally with a sparse vegetation cover during most of the year, rainfall events are often intense and responsible for high erosion and sediment delivery (Langbein and Schumm 1958; Scott 2006). Therefore, an appropriate assessment of the rainfall erosivity is of particular importance due to negative effects caused by nutrients and organic matter depletion (Vörösmarty et al. 2003) and excessive sediment loading to receiving waters to reservoirs (Dutta 2016). In Algeria, with scarce and irregular water resources, sediment delivery ranks among the highest in the word (Probst and Amiotte-Suchet 1992; Megnounif et al. 2003; Achite and Ouillon 2016). According to Meddi et al. (2016), heavy rains threaten 14 million ha of arable land, with consequences that affect the water storage. An average of 45 million m^3 of siltation is deposited each year at the bottom of dams, causing an estimated 0.7% reduction in storage capacity per year (Remini 2008).

Numerous studies investigate the erosivity index (R) presented in different versions of Universal Soil Loss Equation (USLE) (Wischmeier and Smith 1958) to assess the aggressiveness of rainfall as a causal agent of soil erosion (Fournier 1969). Wischmeier and Smith (1978) have described the erosivity of a rainfall event as the result of an energy quantity (E) released when raindrops hit the ground and the maximum

Responsible Editor: Sheryl Luzzadder-Beach

✉ Mourad Guesri
Mouradbox@gmail.com

[1] Research Laboratory Valorisation of Water Resources "V.R.E", Tlemcen University, BP 230, 13000 Tlemcen, Algeria

[2] EOLE Laboratory, Tlemcen University, BP 230, 13000 Tlemcen, Algeria

intensity (I_{30}) of a rainfall event for a period of 30 min. Therefore, a rainfall event is considered an erosive one when the rainfall is effective in terms of sediment yield and the following characteristics are verified: (i) the cumulative rainfall exceeds the threshold $T = 12.7$ mm, without the cumulative rainfall being less than $T/2 = 6.35$ mm for 06 h or (ii) the cumulative rainfall exceeds $T/2 = 6.35$ mm in 15 min. Under these conditions, the evaluation of rainfall erosivity requires rainfall data with a fine temporal resolution, at half an hour or less intervals.

Nevertheless, worldwide, such series are often short, difficult to acquire and time consuming to process as they require the analysis of records from pluviographs (Bertoni and Lombardi Neto 1985). In response to such constraints, alternative solutions are proposed where the R index is explained by easily accessible rainfall data covering long periods such as daily rainfall (Richardson et al. 1983; Choukri et al. 2016; Xie et al. 2016; Beguería et al. 2018; Bouderbala et al. 2019) or monthly (Renard and Freimund 1994; Terranova and Gariano 2015; Ballabio et al. 2017) or annual (Heusch 1970; Bonilla and Vidal 2011; Yin et al. 2015; Toubal et al. 2018). Oduro-Afriyie (1996), Silva (2004) and Fernandez et al. (2019) have associated rainfall erosivity with other precipitation characteristics such as Fournier index (FI) (Fournier 1961) or modified Fournier index (MFI) (Arnoldus 1980), described as:

$$FI = \frac{P_m^2}{P_a}; MFI = \frac{\sum_{i=1}^{12} P_i^2}{P_a} \quad (1)$$

where P_i, P_m and P_a (mm) are the rainfall amount of the ith month; the monthly rainfall of the wettest month and the annual precipitation, respectively. While, Choukri et al. (2016) and Farhan and Alnawaiseh (2018) highlighted the spatiotemporal variability of the rainfall erosivity using annual, seasonal and monthly precipitation.

Soil degradation studies show that sediment load transported by natural streamflow is closely linked to rainfall erosivity (Hicks et al. 2000; Lal 2001) and that the 12.7 mm threshold presented by Wischmeier and Smith (1978) is often excessive (Bollinne 1978; Yin et al. 2017). Denis et al. (2013) adopted an erosive rainfall threshold of 2.5 mm for a semiarid region in India. Mannaerts and Gabriels (2000) have used a threshold of 9 mm to characterise erosive rainfall in Cape Verde, and Xie et al. (2016) have estimated the threshold at 9.7 mm for China. According to McGregor et al. (1995) and Xie et al. (2002), a decrease in the erosive rainfall threshold generates an insignificant increase in the quantification of sediment production.

North of Algeria is a mountainous region characterised by small and medium basin less than 10,000 km^2 with a strong spatiotemporal variability of erosion intensity in response to sparse vegetation and irregular and aggressive climate (Ghenim and Megnounif 2016). In addition to the climate irregularity, the disparity observed between the various rainfall erosivity estimates quoted in the literature review is mainly due to the large panoply of approaches and models used to estimate such parameter. Furthermore, most of the models used were elaborated for distant sites and adapted to local studies, neglecting soil and climate conditions (Meddi et al. 2016; Hasbaia et al. 2017; Toubal et al. 2018; Bouderbala et al. 2019).

This study aims to examine the relationship between rainfall erosivity and sediment production in the Wadi K'sob basin (1480 m^2), which supplies the K'sob dam with an initial capacity of 29.5 Mm^3, commissioned in 1940. The bathymetric survey, carried out in 2010 by the National Agency for Dams and Transfers (ANBT), revealed a high rate of dam alluvium estimated at 67.6%.

The objective of this work is to provide a more accurate overview of the erosive processes that determine sediment yield in the Wadi K'sob watershed, focused on the importance of rainfall in the erosive process and on identifying the effective rainfall threshold in relation to sediment production at seasonal scales. Then, the goal is to develop a model for the study region to estimate the erosivity index from daily rainfall and examine the spatiotemporal variability of erosivity in the study area.

Study area presentation and measurement data

Wadi K'sob, in the northeast of Algeria, drains an area of 1480 km^2 located between altitudes 585 and 1888 m (Fig. 1). The main stream flows over a length of 73 km and supplies the K'sob dam with an initial capacity of 29.5 Mm^3, which was commissioned in 1940. The study area has a semiarid climate with a continental tendency with a relatively wet winter and a dry and hot summer. Most frequent winds come from the northwest, southern winds, in the form of Sirocco, last on average 7 days year^{-1}. Average interannual precipitation is 340 mm. Flow is highly irregular and related to precipitation conditions, with an interannual average of 0.9 m^3 s^{-1}, or an interannual yield of 28 h m^{-3} (Benkadja et al. 2013). Average annual temperature is 15.7 °C. The minimum monthly average, 6.3 °C, is reached in January while the maximum, 27.4 °C, is reached in July.

The study is based on data from five climate stations located throughout the watershed and one hydrometric station located at the outlet of the watershed and upstream of the K'sob dam (Fig. 1). Data are provided by the National Agency for Hydraulic Resources (ANRH). Main information (station name, geographical position

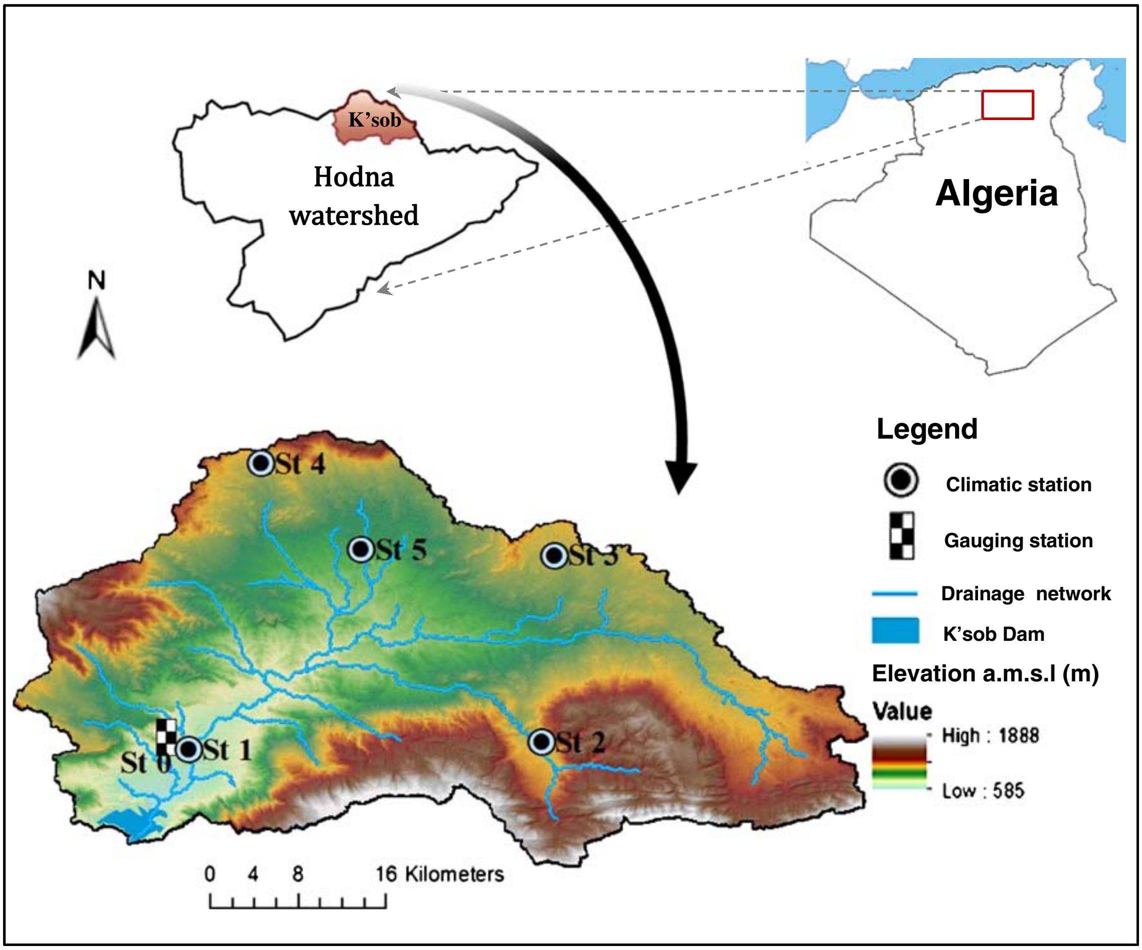

Fig. 1 Watershed overview

and measurement period) is reported in Table 1. Climate stations are equipped with pluviograph and hydrographic stations with a limnimetric ladder and limnigraph. ANRH protocol used to measure water discharge and sediment load is the same in all Algerian regions. Water level is transformed into water discharge using a local abacus updated and checked periodically. For the estimation of the sediment concentration, a water sample is taken from a 1-L vial. Sampling frequency is adapted to the flow regime. It is intensified during high water periods, up to one intake per half hour. Apart from floods, a sample is taken every other day. When flows are very low, a sample is taken every 2 weeks. At each sampling, the supervisor reads the water level to deduce the corresponding flow rate. The suspended solids concentration is estimated in the laboratory by filter weighing according to a protocol

Table 1 Data and measuring stations for precipitation (*P*; mm) discharge (*Q*; m^3/s) and concentration (*C*; g/L)

Station number and name	Latitude	Longitude	Altitude (m)	Period	Time resolution
Rainfall data					
St1 Medjez	35° 53′ 25.78″	4° 037′ 9.27″	636	1973–1994	24 h
St2 Bordj Ghdir	35° 54′ 31.36″	4° 53′ 50.45″	1054	1973–1994	24 h
St3 Sidi Embarek	36° 06′ 5.153″	4° 54′ 31.52″	1021	1973–1994	24 h
St4 Medjana	36° 07′ 44.51″	4° 40′ 26.17″	1042	1973–1994	24 h
St5 Bordj Bouarreridj	35° 59′ 24.23″	4° 45′ 35.26″	922	2007–2015	15 min
Hydrometric data					
St0 Medjez	35° 53′ 25.78″	4° 037′ 9.27″	636	1973–1992	Instant Measurement: *Q* and *C*
				1973–1994	Daily *Q*

detailed in the studies by Achite and Ouillon (2007) and Megnounif et al. (2013).

Methodology

Erosivity estimation

In semiarid regions, soil susceptibility to erosion shows high intra-annual variability in sediment yield (Achite and Ouillon 2016; Choukri et al. 2016; Farhan and Alnawaiseh 2018; Megnounif and Ouillon 2018). To this end, the erosive rainfall threshold characterising Wadi K'sob watershed is sought for the different seasons. Its determination was based on the examination of daily precipitation recorded at the four stations (St1, St2, St3 and St4) during 1973–1992 and where the instantaneous measurement of suspended sediment concentration and discharge was recorded at the gauging station (St0) located at the outlet of the watershed (Table 1). The daily rains recorded at the four stations and occurring until 3 days before a flood event carrying sediment load were examined. In this area, rain may occur locally. Thus, the highest daily rain was considered an erosive rain. After examination of all flood event within a given season, the minimum erosive rain is retained as the threshold of rainfall erosivity.

Once the seasonal thresholds were determined, they were applied to the 15-min rainfall measurements recorded at the station St5 (2007–2015 period) in order to estimate the seasonal erosivity. The selection of erosive rainfall events was done seasonally and following the criteria proposed by Wischmeier and Smith (1978): (i) the cumulative rainfall during a rainfall event must be greater than the seasonal threshold (T) or if (ii) the cumulative rainfall during a 15-min rainfall period, i.e. greater than $T/2$. Cumulative rainfall of less than $T/10$ over a period of 6 h separates the event into two rainfall events. The erosivity of a single rainfall event (R_{Event}) is estimated by the product ($E.I_{30}$), the kinetic energy (E) contained within the rainfall event and (I_{30}, mm h^{-1}) the maximum 30-min intensity during the event.

The parameter E is the total amount of kinetic energy contained within an event and that may entrain the movement of sediment particles; its calculation is given by the following equation:

$$\mathrm{E} = \mathrm{e}_r \mathrm{v}_r \quad (2)$$

where e_r is the unit energy (MJ ha^{-1} mm^{-1}) and v_r the depth of rainfall during a time r. The unit energy was estimated using the formula applied in the Revised Universal Soil Loss Equation (RUSLE) (Brown and Foster 1987):

$$\mathrm{e}_r = 0.29(1-0.72 exp(-0.05 i_r)) \quad (3)$$

where, i_r (mm^{-1} h^{-1}) is the average rainfall intensity over a time interval r.

For each of the four stations (St1, St2, St3 and St4, Table 1), the seasonal erosivity corresponds to the sum of the erosivity of the $R_{\mathrm{Event}} = \mathrm{EI}_{30}$, over a given season:

$$R_s = \sum_{\mathrm{k}=1}^{\mathrm{m_j}} (EI_{30})_k \quad (4)$$

where m_{j} is the number of erosive events within the season under consideration, and EI_{30} is the rainfall erosivity of a single event k.

The annual erosivity is the sum of the erosivity of the four seasons.

Seasonal areal erosivity characterising the Wadi K'sob watershed was deduced using Thiessen's polygon method (de Santos Loureio and Azevedo Coutinho 2001). According to Bruce and Clark (1966), the areal mean obtained using the Thiessen method gives reasonable results for a sparse and unevenly spaced network. While, other methods such as arithmetic mean or isohyetal method require a relatively dense and uniformly spaced rain-gauge network.

Erosivity and sediment production

To each effective rainfall events in terms of sediment yield occurring during the period February 2007 to March 2015 was attributed an R_{Event} and the corresponding daily rain. Then, empirical relationships using simple regression were investigated to simulate the erosivity of rainfall events as a function of daily rain. The relationships between these two parameters were established at seasonal and annual scales. The relevance of the model was examined according to the coefficient of determination. So, the suitable models were used to predict the erosivity of rainfall events. During the period 1973–1994, daily rains exceeding the seasonal rainfall erosivity threshold were introduced in the above models to estimate the erosivity of rainfall events. Then, seasonal and annual erosivity may be computed using Eq.4.

At annual and seasonal scales, the rainfall erosivity was compared with the amount of the suspended sediment yield supplied to the outlet of the watershed. Sediment yield was estimated using a sediment rating curve by performing a linear least-square regression of log-transformed sediment discharge (Q_{s}, kg s^{-1}) against daily water discharge (Q, m^3 s^{-1}). The model is a power function:

$$Q_{\mathrm{s}} = aQ^{b+1} \quad (5)$$

where the parameters a and b are the regression coefficients.

At the gauging station controlling Wadi K'sob, a continuous measure of water level, deduced from a limnigraph, is converted to discharge using a local abacus resulting on the availability of continuous measurements of average daily flows over 1973–1994. Suspended sediment concentration results come from samples collected manually. In addition to some shortcomings observed, it may be suspected that samples were not taken during a brief increasing of discharge at night or during holidays. This justifies the use of the rating curve technique that is widely applied in estimating sediment yield both for small- and large-sized catchments (Walling 1977; Asselman 2000; Horowitz 2003 Warrick 2015; Megnounif and Ghenim 2016).

Over the period 1973–1994, the daily sediment discharges were predicted from the model (Eq. 5) and then used to estimate (Y_S) seasonal sediment yield (Olías et al. 2006; Louamri et al. 2013) using the following formula:

$$Y_s = m \sum_{j=1}^{n} Q_{sd} = m \sum_{j=1}^{n} a \cdot Q_d^{b+1} \quad (6)$$

where $Q_d$and Q_{sd} are the daily water discharge and solid discharge, respectively, m is a constant of unit conversion and n is the number of days par season.

Results

Erosivity threshold

Erosive rainfall event selection criteria applied to data collected between February 2007 and March 2015, identified 134 sediment-effective rainfall events from erosive rainfall thresholds: $T_{autumn} = 3$ mm, $T_{winter} = 6$ mm, $T_{spring} = 2.5$ mm and $T_{summer} = 2$ mm, respectively, for the following seasons: autumn, winter, spring and summer. As a result, these thresholds were compared with the average seasonal rainfall intensity calculated by the equation,

$$I = \frac{4}{n} \sum_{i=1}^{n} P_i \quad (7)$$

where n is the total number of rainfall events per season and P_i the rainfall depth at 15 min time steps. Seasonal evolution shows a negative trend (Fig. 2). Soil erosion susceptibility is minimal in winter, and the average rainfall intensity is low, yielding minimum sediment contribution since the detachment of soil particles has required a high rainfall erosivity threshold. In contrast, in summer and in autumn, soils are more susceptible to erosion and heavy rains result in an important sediment yield.

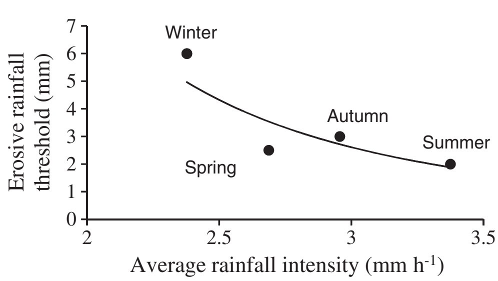

Fig. 2 Seasonal evolution of the rainfall erosivity threshold as a function of average rainfall intensity

Erosivity index

An effective rainfall event in terms of sediment yield is represented by an R_{Event} and the corresponding daily rainfall. Evolution of these two parameters is presented for the different time scales (Fig. 3). According to the coefficients of determination, the relationship is significant at seasonal scales. Indeed, between 68 and 78% of the variance of rainfall erosivity is explained by the daily rainfall giving rise to an erosive rainfall event.

The obtained seasonal models were projected to the 1973–1994 period to estimate rainfall erosivity. Interannual precipitation and erosivity estimated at precipitation stations (Medjaz (St1), Bordj Ghdir (St2), Sidi Embarek (St3) and Medjana (St4)) show an irregular temporal evolution but remain generally similar (Fig. 4). Based on spatial scale, the interannual average of erosivity indices (228, 386, 342 and 255 MJ mm ha^{-1} h^{-1} year^{-1}) was similar to interannual rainfall averages (224, 374, 305 and 284 mm) estimated for each station, respectively.

However, at the stations, Medjaz St1 and Sidi Mebarek St3, rainfall and erosivity were on an upward trend. As a result, average rainfall increased by 1.6 and 3.1 mm year^{-1}, respectively, i.e. in relative value of 0.71–1.41%. This increase remains moderate compared with the average annual increase in erosivity estimated at 6.3 and 10.2 MJ mm ha^{-1} h^{-1} year^{-1}, respectively, a relative increase of 2.8 and 3%. For Bordj Ghdir St2 and Medjana St4 stations, no significant trend was observed except for a slight 1.2% for St2 erosivity.

Rainfall erosivity and sediment production

Regression of solid discharge on water discharge, recorded during the period 1973–1992, takes the form of a power equation (Fig. 5), where 86% of the variance of solid discharge is explained by variation of discharge. Seasonal, in summer and autumn, when the majority of sediment-producing flood events occur, 92% of the variance in solid discharge is explained by water discharge, compared with 85 and 82% in spring and winter (Table 2).

For a multi-year period, sediment yield varies as a function of rainfall erosivity through a power law with a fairly remarkable dispersion around the regression curve equation (Fig. 6). Only 47% of sediment yield variation is explained by rainfall erosivity. Seasonal-scale representation of power models is improving significantly. In autumn, 68% of the variance in sediment yield is explained by rainfall erosivity, compared with 58% in summer, 53% in winter and only 42% in spring.

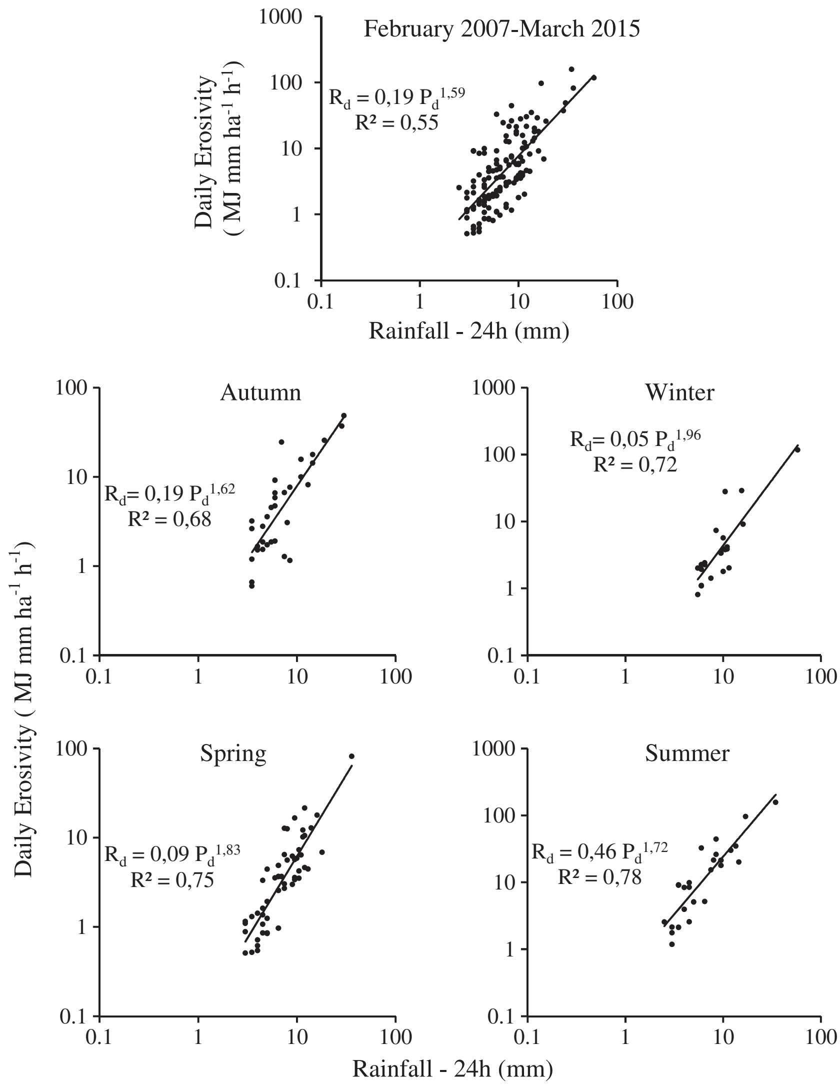

Fig. 3 Rainfall erosivity evolution as a function of daily rainfall at interannual and seasonal scales from February 2007 to March 2015

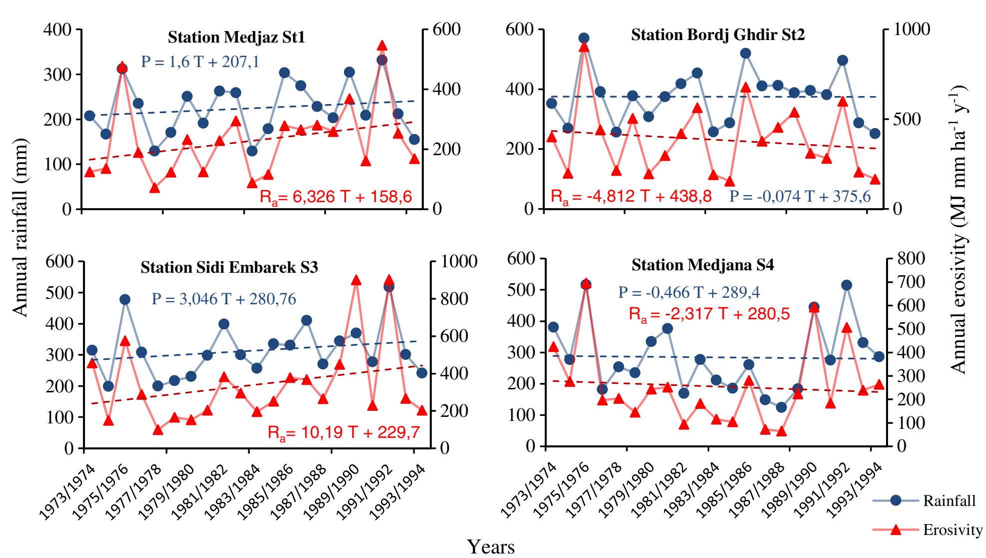

Fig. 4 Interannual evolution of erosivity and precipitation at 4 precipitation stations (1973–1994)

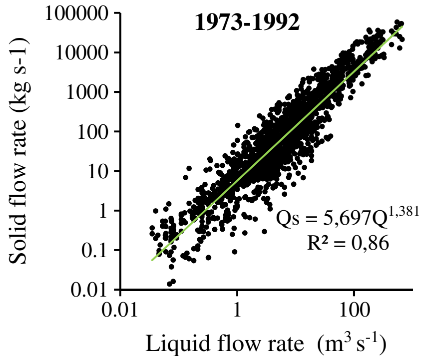

Fig. 5 Regression on solid discharge as a function of water discharge (1973–1992)

Discussion

Rainfall efficiency for sediment yield

Rainfall intensity analysis based on the sediment-producing floods carried by Wadi K'sob allowed to distinguish different thresholds of erosive rainfall for each season. Thresholds identified were in accordance with the nature of the soils in the study region and the semiarid climate with continental influences that prevails in the high plateaus of northern Algeria. The low threshold confirms the high susceptibility of soils to erosion and corroborates the findings of Denis et al. (2013) in semiarid regions in India. During summer and autumn, a low threshold is sufficient because the susceptibility of the soil to erosion is high and the rains are intense. While during winter or spring, a higher threshold is necessary because soils are less favourable to erosion and rains are less intense. Seasonal thresholds identified for Wadi K'sob range from 2 to 6 mm. However, although they were low compared with annual thresholds proposed in the literature (e.g. Bollinne 1978; McGregor et al. 1995; Mannaerts and Gabriels 2000; Xie et al. 2016; Yin et al. 2017) or the 12.7 threshold established by Wischmeier and Smith (1978), the thresholds identified for Wadi k'sob allow a correct estimation of the rainfall erosivity. Between 42 and 68% of the variance of seasonal sediment production is explained by the seasonal average erosivity (Fig. 6). These percentages were considered very significant since sediment production is influenced by several parameters, other than rainfall erosivity, such as rainfall event duration and frequency, temperature variation, land use, cropping practices and human activities (e.g. Walling and Fang 2003; Syvitski et al. 2005; Zhang and Nearing 2005; Walling 2006; Megnounif et al. 2013). Highest percentages correspond to the summer and autumn seasons, when rainfall erosivity is high on dry soils with low vegetation cover (Scott 2006). In spring, only 42% of the variance in sediment production is explained by rainfall erosivity. Indeed, during this time of year, soil is often wet and covered with vegetation, which protects it from eroding rains (Langbein and Schumm 1958; Seeger et al. 2004). On the other hand, these percentages indicate that in this region, rainfall eruption is the determining factor in sediment production as reported in several studies conducted on sediment production in semiarid climates (e.g. Langbein and Schumm 1958; Scott 2006).

Table 2 Seasonal Q_s-Q models, number of observations 'No. Obs' and coefficient of determination (R^2) (1973–1992)

Season	No. Obs	R^2	Models
Autumn	580	0.92	$Q_s = 8.066\ Q^{1.435}$
Winter	341	0.85	$Q_s = 3.779\ Q^{1.361}$
Spring	478	0.82	$Q_s = 3.655\ Q^{1.364}$
Summer	247	0.92	$Q_s = 9.485\ Q^{1.373}$

Erosivity estimation models validation

From February 2007 to March 2015, the rainfall record at 15-min intervals was used to calculate the annual R-RUSLE erosivity using the approach established in the RUSLE (Renard et al. 1997).

Deduced results were compared with the annual erosivity (R-Model) estimated by both this study and other models in the literature and commonly used. This comparison is introduced as a criterion for assessing the quality of the models to be used to estimate the annual erosivity of rainfall. To this purpose, a simple linear regression is established between the R-RUSLE and R-model points as shown in Fig. 7. A 'good' model is one that gives a straight line with a slope close to 1 and an affix close to 0. For example, the closer the coefficient of determination is to 1, the more points where the R-Model estimate is in good agreement with the R-RUSLE estimate. When the coefficient of determination is close to 1, the slope of the regression line indicates whether the model underestimates or overestimates the R-RUSLE erosivity.

Based on these criteria, the model proposed in this study has the highest performance to approach the R-RUSLE erosivity estimates with an average underestimation of around 6%. However, the models established by Ávila and Ávila (2015) and Elangovan and Seetharaman (2011) underestimate R-RUSLE erosivity by 33 to 78%, respectively. Models proposed by Sanchez-Moreno et al. (2014), Mannaerts and Gabriels (2000) and Lee and Lin (2015) overestimate R-RUSLE erosivity between 49 and 138%.

Rainfall and annual erosivity spatiotemporal variability

On an interannual scale, erosivity and rainfall show similar fluctuations. Seasonal differences were identified in

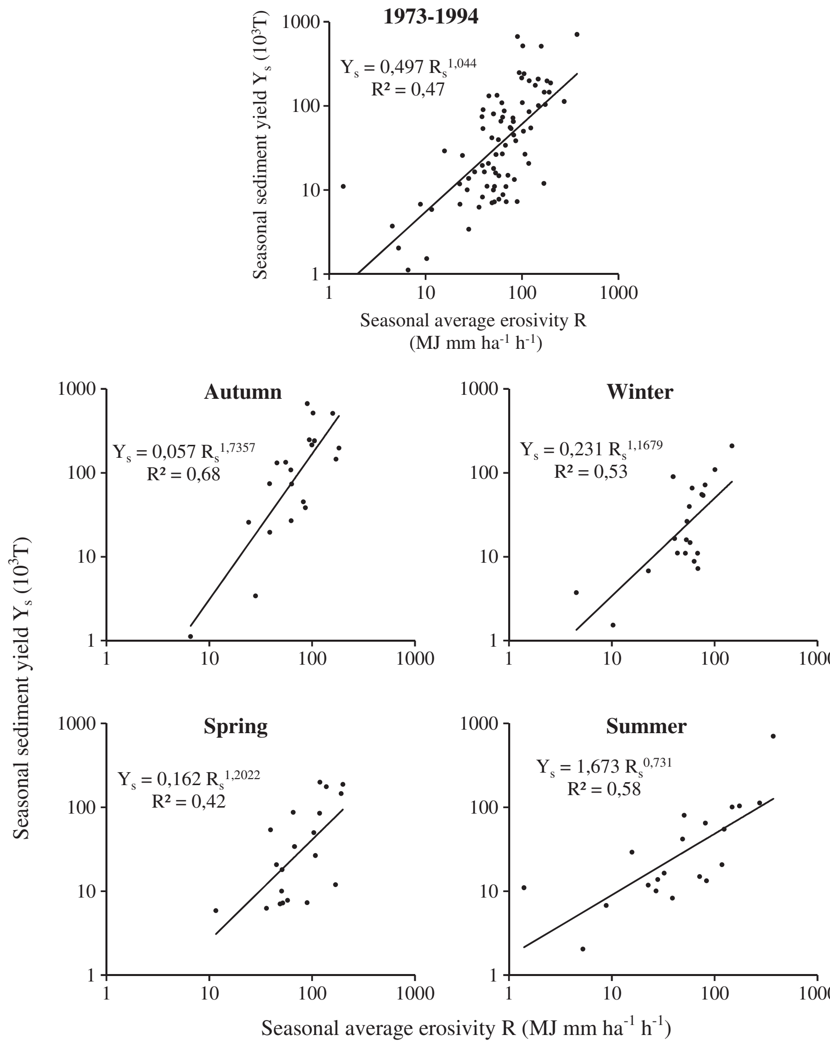

Fig. 6 Rainfall erosivity related to sediment yield

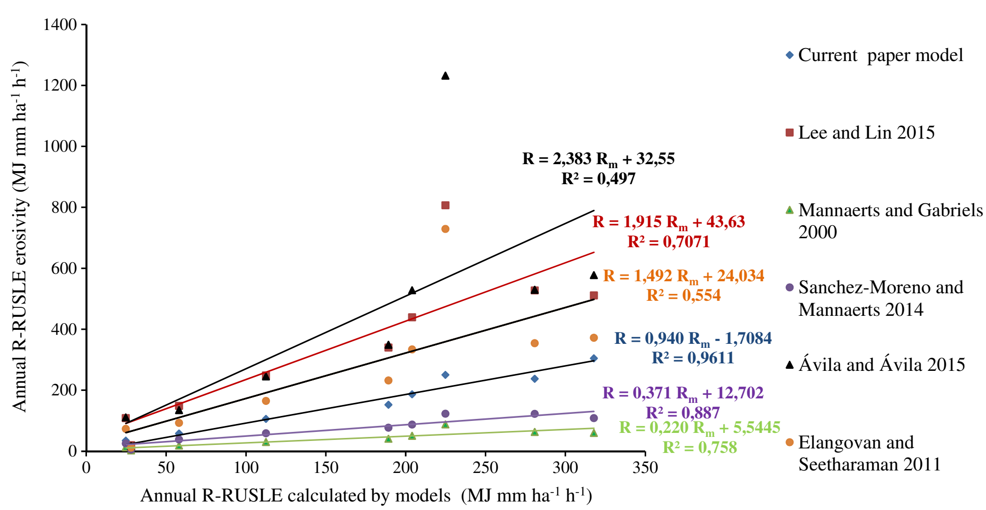

Fig. 7 Comparison between R-RUSLE-estimated values based on daily rainfall models

Table 3 Spatial and seasonal distribution of rainfall erosivity density (%)

	St1 Medjaz	St2 Bordj Ghdir	St3 Sidi Embarek	St4 Medjana
Autumn	89.65	87.91	91.94	94.32
Winter	72.13	73.62	72.12	66.67
Spring	92.28	91.91	95.24	98.45
Summer	91.97	92.88	98.22	89.59

erosivity density estimated by the rainfall erosivity quotient (Panagos et al. 2016; Ballabio et al. 2017). The highest densities were recorded during the summer and spring seasons, at the four stations, St1, St2, St3 and St4, when they ranged from 89 to 98%, as indicated in Table 3. In autumn and winter, they fluctuate between 87 and 94% and 66 and 74%, respectively. Overall, erosivity density remains high and appears to be closely related to annual rainfall intensity, as shown in Fig. 2. In terms of spatial variability, erosivity index is mainly associated with rainfall abundance, as illustrated in Fig. 8. Table 3 indicates that erosivity density remains almost spatially similar in rainfall.

The annual spatial average of erosivity in Wadi K'sob watershed varies between 228 and 386 MJ mm ha^{-1} h^{-1} $year^{-1}$. The interannual average is 302 MJ mm ha^{-1} h^{-1} $year^{-1}$. In the same basin, the Yu and Rosewell (1996) model, adopted by Benkadja et al. (2015), gives interannual estimates 24 to 45% lower than those established in this study, as indicated in Table 4. In comparison with the interannual erosivity estimates for northern Maghreb, estimates carried out in this study were within the range proposed for northern Algeria by Meddi et al. (2016) and remain moderate compared with those for Wadi Mina in Algeria (Benchettouh et al. 2017) and Boulabbouz in Tunisia (Kefi and Yoshino 2010). Meanwhile, Table 4 indicates that research conducted in other Maghreb countries provides relatively low estimates for rainfall erosivity.

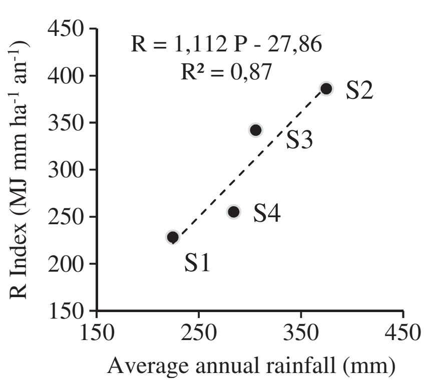

Fig. 8 Erosivity spatial variation based on annual rainfall

Table 4 Sample estimation of rainfall erosivity index in Maghreb countries

Country	Study area	*R* (MJ mm ha^{-1} h^{-1} $year^{-1}$)	Author
Algeria	Northern Algeria	200–1000	Meddi et al. (2016)
	Oued Mina	370–773	Benchettouh et al. (2017)
	Bv Bouhamdane	160–240	Bouguerra et al. (2017)
	Sebaa Chioukh's mounts	62–87	Meghraoui et al. (2017)
	Centre Bv Aurès	47–192	Hassen et al. (2017)
	Bv K'sob	125–292	Benkadja et al. (2015)
Morocco	Bv Kalaya	95–100	Issa et al. (2016)
	Bv Ourika	55–100	Meliho et al. (2016)
	BV de Tahaddart	33–46	Tahiri et al. (2014)
Tunisia	BV Oued El Sourrag	33–38	Medhioub et al. (2017)
	Bv Lebna	73–95	Gaubi et al. (2017)
	Bv Boulabbouz	396	Kefi and Yoshino (2010)

Conclusion

The study was conducted in Wadi K'sob basin (1480 km^2) in northeast Algeria. This region has a semi-arid climate with continental influence. A model was developed to estimate the erosivity index based on daily rainfall. The integration of distinct erosive rainfall thresholds for each season into the model allowed consideration of intra-annual variability in rainfall and changes in soil conditions.

Erosive rainfall thresholds were established based on sediment yield. During summer and autumn seasons, rainfall is often heavy and soil particulates are more susceptible to detachment. During this time of year, erosive rainfall is low. On the other hand, winter rains are less intense and require a higher threshold to cause the particles to detach from the soil. A model for estimating the erosivity index as a function of daily rainfall was developed.

The study reveals a spatiotemporal similarity between the erosivity index and rainfall. The relationship is close during the summer and autumn seasons when the rains are intense. Similarly, the study shows that rainfall erosivity is the determining factor in sediment production with a different degree of binding during the year. In autumn, 68% of the variance in sediment production is explained by rainfall erosivity, compared with only 42% in spring due to changes in soil conditions, including the presence of a vegetation cover that protects the soil from rainfall erosivity.

References

Achite M, Ouillon S (2007) Suspended sediment transport in a semiarid watershed, Wadi Abd, Algeria (1973-1995). J Hydrol 343:187–202. https://doi.org/10.1016/j.jhydrol.2007.06.026

Achite M, Ouillon S (2016) Recent changes in climate, hydrology and sediment load in the Wadi Abd, Algeria (1970-2010). Hydrol Earth Syst Sci 20:1355–1372. https://doi.org/10.5194/hess-20-1355-2016

Arnoldus HMJ (1980) An approximation of the rainfall factor in the Universal Soil Loss Equation. In: De Boodt M, Gabriels D (eds) Assessment of erosion. Wiley, Chichester, pp 127–132

Asselman NEM (2000) Fitting and interpretation of sediment rating curves. J Hydrol 234:228–248. https://doi.org/10.1016/S0022-1694(00)00253-5

Ávila B, Ávila H (2015) Spatial and temporal estimation of the erosivity factor R based on daily rainfall data for the department of Atlántico, Colombia. Ing Investig 35:23–29. https://doi.org/10.15446/ing.investig.v35n2.47773

Ballabio C, Borrelli P, Spinoni J et al (2017) Mapping monthly rainfall erosivity in Europe. Sci Total Environ 579:1298–1315

Beguería S, Serrano-Notivoli R, Tomas-Burguera M (2018) Computation of rainfall erosivity from daily precipitation amounts. Sci Total Environ 637:359–373

Benchettouh A, Kouri L, Jebari S (2017) Spatial estimation of soil erosion risk using RUSLE/GIS techniques and practices conservation suggested for reducing soil erosion in Wadi Mina watershed (northwest, Algeria). Arab J Geosci 10. https://doi.org/10.1007/s12517-017-2875-6

Benkadja R, Benhadouga M, Benkadja A (2013) Quantification des matières en suspension et valorisation des sédiments de dragage à l'échelle d'un bassin semi-aride: Cas du barrage du K'sob (Algérie). Bull Eng Geol Environ 72:523–531. https://doi.org/10.1007/s10064-013-0516-1

Benkadja R, Boussag F, Benkadja A (2015) Identification et évaluation du risque d'érosion sur le bassin versant du K'sob (Est Algérien). Bull Eng Geol Environ 74:91–102. https://doi.org/10.1007/s10064-014-0611-y

Bertoni J, Lombardi Neto F (1985) Conservação do solo, 3rd edn. Ícone, São Paulo, Brasil, p 355

Bollinne A (1978) Study of the importance of splash and wash on cultivated loamy soils of Hesbaye (Belgium). Earth Surf Process 3:71–84

Bonilla CA, Vidal KL (2011) Rainfall erosivity in Central Chile. J Hydrol 410:126–133. https://doi.org/10.1016/j.jhydrol.2011.09.022

Bouderbala D, Souidi Z, Hamimed A, Bouamar B (2019) Estimation of rainfall erosivity by mapping at the watershed of macta (Algeria). Rev Bras Cart 71:274–294

Bouguerra H, Bouanani A, Khanchoul K et al (2017) Mapping erosion prone areas in the Bouhamdane watershed (Algeria) using the Revised Universal Soil Loss Equation through GIS. J Water Land Dev 32:13–23. https://doi.org/10.1515/jwld-2017-0002

Brown LC, Foster GR (1987) Storm erosivity using idealized intensity distributions. Trans ASAE 30:379–386

Bruce JP, Clark RH (1966) Introduction to hydrometeorology. Pergamon Press, Long Island City, NY

Choukri F, Chikhaoui M, Naimi M et al (2016) Impact Du Changement Climatique Sur L'évolution De L'érosivité Des Pluies Dans Le Rif Occidental (Nord Du Maroc). Eur Sci Journal, ESJ 12

Da Silva AM (2004) Rainfall erosivity map for Brazil. Catena 57:251–259. https://doi.org/10.1016/j.catena.2003.11.006

De Santos Loureiro N, De Azevedo Coutinho M (2001) A new procedure to estimate the RUSLE EI30index, based on monthly rainfall data and applied to the Algarve region, Portugal. J Hydrol 250:12–18. https://doi.org/10.1016/S0022-1694(01)00387-0

Denis MKA, Patil PL, Dasog GS, Manjunath MV (2013) Rainfall erosivity (R-factor) estimation for Singhanalli-Bogur micro-watershed in northern transition zone of Karnataka. Res J Agric Sci 4:644–647

Dutta S (2016) Soil erosion, sediment yield and sedimentation of reservoir: a review. Model Earth Syst Environ 2:123

Elangovan A, Seetharaman R (2011) Estimating rainfall erosivity of the Revised Universal Soil Loss Equation from daily rainfall depth in Krishanagiri watershed region of Tamil Nadu. India Int Conf 19:48–52. https://doi.org/10.1016/j.cjca.2015.11.019

Farhan Y, Alnawaiseh S (2018) Spatio-temporal variation in rainfall erosivity over Jordan using annual and seasonal precipitation. Nat Resour 9:242

Fernandez H, Martins F, Isidoro JMGP (2019) Mapping rainfall aggressiveness from physiographical data: application to the Grândola Mountain range (Alentejo, Portugal). Phys Geogr:1–16

Fournier F (1961) Climat et erosion. Soil Sci 92:151

Fournier F (1969) L'érosion hydrique et le climat. Bulletin technique d'information

Gaubi I, Chaabani A, Ben Mammou A, Hamza MH (2017) A GIS-based soil erosion prediction using the Revised Universal Soil Loss Equation (RUSLE) (Lebna watershed, Cap Bon, Tunisia). Nat Hazards 86:219–239. https://doi.org/10.1007/s11069-016-2684-3

Ghenim AN, Megnounif A (2016, 2016) Variability and trend of annual maximum daily rainfall in northern Algeria. Int J Geophys. https://doi.org/10.1155/2016/6820397

Hasbaia M, Zeroual S, Dougha M et al (2017) Prediction of dams silting in semi-arid region using erosion map under GIS environment, case of Ksob watershed in Hodna Region (Algeria). In: Euro-Mediterranean Conference for Environmental Integration. Springer, pp 781–783

Hassen B, Soufiane L, Chaouki C (2017) Mapping and modelling of areas at risk of erosion: case of Aures Center (Algeria). In: Water resources in arid areas: the way forward. Springer, pp 197–214

Heusch B (1970) Estimation et controle de l'érosion hydraulique. Soc ScPhys Maroc 1970. N spécial, pp. 41–54

Hicks DM, Gomez B, Trustrum NA (2000) Erosion thresholds and suspended sediment yields, Waipaoa River basin, New Zealand. Water Resour Res 36:1129–1142

Horowitz AJ (2003) An evaluation of sediment rating curves for estimating suspended sediment concentrations for subsequent flux calculations. Hydrol Process 17:3387–3409

Issa LK, Lech-Hab KBH, Raissouni A, El Arrim A (2016) Cartographie quantitative du risque d'erosion des sols par approche SIG/USLE au niveau du bassin versant kalaya (Maroc Nord Occidental). J Mater Environ Sci 7:2778–2795

Kefi M, Yoshino K (2010) Evaluation of the economic effects of soil erosion risk on agricultural productivity using remote sensing: case of watershed in Tunisia. Int Arch Photogramm Remote Sens Spat Inf Sci—ISPRS Arch 38:930–935

Lal R (2001) Soil degradation by erosion. Land Degrad Dev 12:519–539

Langbein WB, Schumm SA (1958) Yield of sediment in relation to mean annual precipitation. EOS Trans Am Geophys Union 39:1076–1084

Lee MH, Lin HH (2015, 2015) Evaluation of annual rainfall erosivity index based on daily, monthly, and annual precipitation data of rainfall station network in Southern Taiwan. Int J Distrib Sens Netw. https://doi.org/10.1155/2015/214708

Louamri A, Mebarki A, Laignel B (2013) Variabilité interannuelle et intra-annuelle des transports solides de l'Wadi Bouhamdane, à l'amont du barrage Hammam Debagh (Algérie orientale). Hydrol Sci J 58:1559–1572. https://doi.org/10.1080/02626667.2013.824089

Mannaerts CM, Gabriels D (2000) Rainfall erosivity in Cape Verde. Soil Tillage Res 55:207–212. https://doi.org/10.1007/BF00118052

McGregor KC, Bingner RL, Bowie AJ, Foster GR (1995) Erosivity index values for northern Mississippi. Trans ASAE 38:1039–1047

Meddi M, Toumi S, Assani AA (2016) Spatial and temporal variability of the rainfall erosivity factor in northern Algeria. Arab J Geosci 9:1–13. https://doi.org/10.1007/s12517-015-2303-8
Medhioub E, Bouaziz M, Bouaziz S (2017) Assessment of soil erosion by water using RUSLE, remote sensing and GIS in Gabes Coast-Southern Tunisia: study case of Wadi El Sourrag watershed. In: Euro-Mediterranean Conference for Environmental Integration. Springer, pp 1805–1806
Meghraoui M, Habi M, Morsli B et al (2017) Mapping of soil erodibility and assessment of soil losses using the RUSLE model in the Sebaa Chioukh Mountains (northwest of Algeria). J Water Land Dev 34: 205–213. https://doi.org/10.1515/jwld-2017-0055
Megnounif A, Ghenim AN (2016) Rainfall irregularity and its impact on the sediment yield in Wadi Sebdou watershed, Algeria. Arab J Geosci 9:1–15. https://doi.org/10.1007/s12517-015-2280-y
Megnounif A, Ouillon S (2018) Empirical and analytical methods to characterize the efficiency of floods to move sediment in a small semi-arid basin. Hydrol Earth Syst Sci 22:6335–6355. https://doi.org/10.5194/hess-22-6335-2018
Megnounif A, Terfous A, Bouanani A (2003) Production et transport des matières solides en suspension dans le bassin versant de la Haute-Tafna (Nord-Ouest Algérien). Rev Sci L'eau 16:369. https://doi.org/10.7202/705513ar
Megnounif A, Terfous A, Ouillon S (2013) A graphical method to study suspended sediment dynamics during flood events in the Wadi Sebdou, NW Algeria (1973-2004). J Hydrol 497:24–36. https://doi.org/10.1016/j.jhydrol.2013.05.029
Meliho M, Khattabi A, Mhammdi N, Hongming Z (2016) Impact of land use and vegetation cover on risks of erosion in the Ourika watershed (Morocco). Am J Eng Res (AJER):75–82
Oduro-Afriyie K (1996) Rainfall erosivity map for Ghana. Geoderma 74: 161–166. https://doi.org/10.1016/S0016-7061(96)00054-7
Olías M, Cánovas CR, Nieto JM, Sarmiento AM (2006) Evaluation of the dissolved contaminant load transported by the Tinto and Odiel rivers (South West Spain). Appl Geochem 21:1733–1749
Panagos P, Ballabio C, Borrelli P, Meusburger K (2016) Spatio-temporal analysis of rainfall erosivity and erosivity density in Greece. Catena 137:161–172. https://doi.org/10.1016/j.catena.2015.09.015
Probst JL, Amiotte-Suchet P (1992) Fluvial suspended sediment transport and mechanical erosion in the Maghreb (North Africa). Hydrol Sci J 37:621–637. https://doi.org/10.1080/02626669209492628
Remini B (2008) La surélévation des barrages: une technique de lutte contre l'envasement-exemples algériens. La Houille Blanche:103–108
Renard KG, Freimund JR (1994) Using monthly precipitation data to estimate the R-factor in the revised USLE. J Hydrol 157:287–306. https://doi.org/10.1016/0022-1694(94)90110-4
Renard KG, Foster GR, Weesies GA, McCool DK, Yoder DC (1997) Predicting soil erosion by water: a guide to conservation planning with the Revised Universal Soil Loss Equation (RUSLE). U.S. Government Printing Office, USA
Richardson CW, Foster GR, Wright DA (1983) Estimation of erosion index from daily rainfall amount. Trans ASAE 26(1):153–156
Sanchez-Moreno JF, Mannaerts CM, Jetten V (2014) Rainfall erosivity mapping for Santiago Island, Cape Verde. Geoderma 217–218:74–82. https://doi.org/10.1016/j.geoderma.2013.10.026
Scott SH (2006) Predicting sediment transport dynamics in ephemeral channels: a review of literature. Engineer Research and Development Center Vicksburg Ms Coastal and Hydraulics Lab
Seeger M, Errea M-P, Beguerıa S et al (2004) Catchment soil moisture and rainfall characteristics as determinant factors for discharge/suspended sediment hysteretic loops in a small headwater catchment in the Spanish Pyrenees. J Hydrol 288:299–311
Syvitski JPM, Vörösmarty C, Kettner AJ, Green P (2005) Impact of humans on the flux of terrestrial sediment to the global coastal ocean. Science 308:376–380
Tahiri M, Tabyaoui H, El Hammichi F et al (2014) Evaluation et quantification de l'érosion et la sédimentation à partir des modèles RUSLE, MUSLE et Déposition intégrés dans un SIG. Application au sous bassin de l'Wadi Sania (Bassin de Tahaddart, Rif nord occidental, Maroc). Eur J Sci Res 125:157–178
Terranova OG, Gariano SL (2015) Regional investigation on seasonality of erosivity in the Mediterranean environment. Environ Earth Sci 73:311–324
Toubal AK, Achite M, Ouillon S, Dehni A (2018) Soil erodibility mapping using the RUSLE model to prioritize erosion control in the Wadi Sahouat basin, North-West of Algeria. Environ Monit Assess 190:1–22. https://doi.org/10.1007/s10661-018-6580-z
Vörösmarty CJ, Meybeck M, Fekete B et al (2003) Anthropogenic sediment retention: major global impact from registered river impoundments. Glob Planet Chang 39:169–190
Walling DE (1977) Assessing the accuracy of suspended sediment rating curves for a small basin. Water Resour Res 13:531–538
Walling DE (2006) Human impact on land–ocean sediment transfer by the world's rivers. Geomorphology 79:192–216. https://doi.org/10.1016/j.geomorph.2006.06.019
Walling DE, Fang D (2003) Recent trends in the suspended sediment loads of the world's rivers. Glob Planet Chang 39:111–126
Warrick JA (2015) Trend analyses with river sediment rating curves. Hydrol Process 29:936–949
Wischmeier WH, Smith DD (1958) Rainfall energy and its relationship to soil loss. EOS Trans Am Geophys Union 39:285–291. https://doi.org/10.1029/TR039i002p00285
Wischmeier WH, Smith DD (1978) Predicting rainfall erosion losses. USDA agricultural research services handbook 537. USDA, Washington, DC, 57pp
Xie Y, Liu B, Nearing MA (2002) Practical thresholds for separating erosive and non-erosive storms. Trans ASAE (American Soc Agric Eng) 45:1843–1847
Xie Y, Yin SQ, Liu BY et al (2016) Models for estimating daily rainfall erosivity in China. J Hydrol 535:547–558
Yin S, Xie Y, Liu B, Nearing MA (2015) Rainfall erosivity estimation based on rainfall data collected over a range of temporal resolutions. Hydrol Earth Syst Sci 19:4113–4126. https://doi.org/10.5194/hess-19-4113-2015
Yin S, Nearing MA, Borrelli P, Xue X (2017) Rainfall erosivity: an overview of methodologies and applications. Vadose Zo J 16:0. https://doi.org/10.2136/vzj2017.06.0131
Yu B, Rosewell CJ (1996) Rainfall erosivity estimation using daily rainfall amounts for South Australia. Aust J Soil Res 34:721–733. https://doi.org/10.1071/SR9960721
Zhang XC, Nearing MA (2005) Impact of climate change on soil erosion, runoff, and wheat productivity in Central Oklahoma. Catena 61(2): 185–195